IAI Journals.ASM.org

Nonreplicating, Cyst-Defective Type II *Toxoplasma gondii* Vaccine Strains Stimulate Protective Immunity against Acute and Chronic Infection

Barbara A. Fox, David J. Bzik

Department of Microbiology and Immunology, Geisel School of Medicine at Dartmouth, Lebanon, New Hampshire, USA

Live attenuated vaccine strains, such as type I nonreplicating uracil auxotroph mutants, are highly effective in eliciting lifelong immunity to virulent acute infection by *Toxoplasma gondii*. However, it is currently unknown whether vaccine-elicited immunity can provide protection against acute infection and also prevent chronic infection. To address this problem, we developed nonreverting, nonreplicating, live attenuated uracil auxotroph vaccine strains in the type II Δ*ku80* genetic background by targeting the deletion of the orotidine 5′-monophosphate decarboxylase (*OMPDC*) and uridine phosphorylase (*UP*) genes. Deletion of *OMPDC* induced a severe uracil auxotrophy with loss of replication, loss of virulence in mice, and loss of the ability to develop cysts and chronic infection. Vaccination of mice using type II Δ*ku80* Δ*ompdc* mutants stimulated a fully protective CD8$^+$ T cell-dependent immunity that prevented acute infection by type I and type II strains of *T. gondii*, and this vaccination also severely reduced or prevented cyst formation after type II challenge infection. Nonreverting, nonreplicating, and non-cyst-forming Δ*ompdc* mutants provide new tools to examine protective immune responses elicited by vaccination with a live attenuated type II vaccine.

Toxoplasma gondii is an obligate intracellular parasite with an extremely broad host range inclusive of most birds and virtually all mammals (1). *T. gondii* chronically infects approximately one-third of the human population (2). Three major strain types are found in North America and Europe, and these type I, II, or III strains differ with respect to their virulence traits in mice (3). Type I strains are considered to be highly virulent, type II strains have low virulence, and type III strains are considered to be avirulent. Following acute infection by type II strains of *T. gondii*, a chronic infection is established. Chronic infection is characterized by slow-growing bradyzoite forms within tissue cysts in brain, muscle, and eye (4), and infection is considered to be lifelong (5, 6). Reactivated infection during AIDS or immune suppression may cause a severe and difficult to treat toxoplasmic encephalitis (7) or recurrent ocular toxoplasmosis (8). Vaccination against *Toxoplasma* is difficult due to the existence of multiple antigenically distinct strain types and multiple antigenically distinct developmental stages. *Toxoplasma* also can effectively escape immunity by the development of a chronic encysted stage that is not easily cleared by immune responses.

Antigen-based vaccine formulations provide only a partially protective immunity and do not prevent the establishment of tissue cysts and chronic infection following exposure to *T. gondii* (9). Immunization with *T. gondii* extracts or killed noninvasive parasites also fails to elicit significant immunity to reinfection with *T. gondii* (10, 11). Suboptimal vaccine priming using antigen-based vaccine formulations is not surprising in view of the requirement for populations of CD8$^+$ and CD4$^+$ T cells that produce the interferon gamma (IFN-γ) that is necessary to establish immunity and control of natural infection (12). In contrast to the suboptimal immunity elicited by antigen-based vaccines, immunization with whole transgenic organisms elicits potent Th1-biased immune responses associated with control of infection, and this vaccination strategy has enabled key experimental insights into host responses that prime immunity (13).

Disruption of the *de novo* pyrimidine synthesis pathway has led to remarkably effective vaccination strategies based on live attenuated uracil auxotroph vaccine strains (14). Disruption of carbamoyl phosphate synthetase II in the virulent type I RH strain (the CPS mutant) induced a severe uracil auxotrophy (15, 16). CPS is a live attenuated mutant that invades host cells normally but fails to proliferate within its vacuole due to nutrient limitation, and this loss of replication ability causes a complete absence of virulence during infection (15). Disruption of the orotidine 5′-monophosphate decarboxylase gene (*OMPDC*) in the virulent type I RH Δ*ku80* strain (17) also produced a nonreplicating uracil auxotroph mutant that elicited protective immunity to virulent acute infection (18). The extreme attenuation and avirulence of type I *T. gondii* uracil auxotrophs are exemplified by survival of severely immune-deficient IFN-γ$^{-/-}$ knockout mice (15, 18, 19) and interleukin-2 receptor γ knockout (NOD/SCID/IL-2Rγ$^{-/-}$) mice (20) that were infected with high-dose challenges of CPS.

Vaccination with CPS elicits a lifelong CD8$^+$ T cell-dependent immunity against infection with type I strains (15, 18, 19, 21, 22). This immunity is also effectively elicited in *tyk2*$^{-/-}$ (23) or in

Received 6 October 2014 **Returned for modification** 24 November 2014
Accepted 6 March 2015

Accepted manuscript posted online 16 March 2015

Citation Fox BA, Bzik DJ. 2015. Nonreplicating, cyst-defective type II *Toxoplasma gondii* vaccine strains stimulate protective immunity against acute and chronic infection. Infect Immun 83:2148–2155. doi:10.1128/IAI.02756-14.

Editor: J. H. Adams

Address correspondence to Barbara A. Fox, barbara.a.fox@dartmouth.edu, or David J. Bzik, david.j.bzik@dartmouth.edu.

Supplemental material for this article may be found at http://dx.doi.org/10.1128/IAI.02756-14.

doi:10.1128/IAI.02756-14

MyD88$^{-/-}$ signaling-deficient mice (24). Immunity elicited by vaccination with CPS requires production of interleukin-12 (IL-12) (24, 25), IFN-γ (15, 19), and CD8$^+$ T cell populations (25, 26), which possess cytolytic activity *in vitro* and *in vivo* (22). Previous studies have implicated a key role for active *T. gondii* invasion of host cells in mechanisms that promote T cell immunity to *Toxoplasma* (27–29). Recent studies using the CPS vaccination model have found a role for active parasite invasion in the activation of myeloid cells and the priming of CD4$^+$ and CD8$^+$ T cell immunity (30–32). Furthermore, phagocytosis of CPS by myeloid cells elicited surprisingly insignificant CD4$^+$ and CD8$^+$ T cell responses and ineffective immunity to *Toxoplasma* (21). In contrast, active invasion of myeloid cells by CPS triggered potent CD4$^+$ and CD8$^+$ T cell responses and highly effective protective immunity to *Toxoplasma* (21).

Previously, vaccination with CPS was shown to protect mice against a virulent acute infection after challenge with a type I or type II strain of *T. gondii*. However, this CPS vaccination did not completely prevent the development of cysts and chronic infection in mice that were challenged with a type II strain (33). Here, we developed nonreverting uracil auxotroph vaccine strains in the type II Δ*ku80* genetic background by deleting the orotidine 5′-monophosphate decarboxylase gene (*OMPDC*). The resulting type II Pru Δ*ku80* Δ*ompdc* mutants exhibit a severe uracil auxotrophy with loss of replication and virulence and undetectable cyst formation. Vaccination of mice with the type II Pru Δ*ku80* Δ*ompdc* mutant stimulates a potent protective immunity against infection by type I and type II strains of *Toxoplasma gondii*.

MATERIALS AND METHODS

Primers. All oligonucleotide primers used in this study for plasmid construction and PCR validation of genotypes of mutant strains are listed in Tables S1 and S2 in the supplemental material.

Plasmid constructs. Yeast recombination was used to fuse 3 distinct genetic elements (a 5′ target flank, a hypoxanthine-xanthine-guanine phosphoribosyltransferase gene [*HXGPRT*] selectable marker, and a 3′ target flank) in their correct order in the yeast shuttle plasmid vector pRS416. This recombination was performed using 29- to 36-bp crossovers common to pRS416 and the *HXGPRT* selectable marker or to the gene targeting flanks (see Table S1 in the supplemental material) (18, 34). Gene knockout targeting plasmids were engineered to delete a short region of the gene's predicted 5′ untranslated region (UTR) and the entire predicted coding region of the targeted genomic locus (www.ToxoDB.org, version 12.0). Targeting plasmids were first verified by restriction enzyme digest and were sequenced to verify 100% gene homology to the available type II ME49 genome sequence (17).

Plasmid pOMPP4 was constructed to delete nucleotides 2709536 to 2712859 in the *OMPDC* locus defined as TGME49_259690 (55.m04842) on chrVIIb of the ToxoDB database. The *HXGPRT* minigene cassette (35, 36) was fused between a 1,055-bp 5′ genomic targeting flank and a 994-bp 3′ genomic targeting flank amplified from DNA isolated from the Pru Δ*ku80*::*HXGPRT* strain (37).

Plasmid pOMPPC4 was constructed to remove *HXGPRT* from the disrupted chromosomal *OMPDC* locus of the Pru Δ*ku80* Δ*ompdc*::*HXGPRT* strain. Plasmid pOMPP4 was digested with PmeI to remove the *HXGPRT* cassette fragment followed by self-religation.

Plasmid pNUPP3 was designed to delete nucleotides 1497792 to 1500995 of the uridine phosphorylase (*UP*) locus on chrXI annotated as TGME49_310640. The *HXGPRT* minigene cassette was fused between a 1,024-bp 5′ targeting fragment and a 934-bp 3′ targeting fragment.

Plasmid pgUPROMP was designed to complement uracil auxotrophy while disrupting the uracil phosphoribosyltransferase locus (*UPRT*). A chromosomal segment of 3,258 bp corresponding to nucleotides 2712430 to 2709172 (−) on chrVIIb (the *OMPDC* gene) was flanked with a 1,151-bp 5′ *UPRT* targeting DNA flank and a 1,119-bp 3′ *UPRT* targeting DNA flank. Plasmid pGUPROMT was designed to replace nucleotides corresponding to 2718655 to 2722697 of the annotated *UPRT* chromosomal locus TGME49_312480 chrXI.

TABLE 1 Strains used in this study

Strain characteristic(s)	Parent strain characteristic(s)	Source or reference
RH	RH(ERP)	38, 41
RH Δ*ku80* Δ*ompdc*::*HXGPRT*	RH Δ*ku80* Δ*hxgprt*	18
Pru Δ*ku80*::*HXGPRT*	Pru Δ*hxgprt*	37
Pru Δ*ku80* Δ*hxgprt*	Pru Δ*ku80*::*HXGPRT*	37
Pru Δ*ku80* Δ*ompdc*::*HXGPRT*	Pru Δ*ku80* Δ*hxgprt*	This study
Pru Δ*ku80* Δ*up*::*HXGPRT*	Pru Δ*ku80* Δ*hxgprt*	This study
Pru Δ*ku80* Δ*ompdc* Δ*hxgprt*	Pru Δ*ku80* Δ*ompdc*::*HXGPRT*	This study
Pru Δ*ku80* Δ*ompdc* Δ*up*::*HXGPRT*	Pru Δ*ku80* Δ*ompdc* Δ*hxgprt*	This study
Pru Δ*ku80* Δ*ompdc*::*HXGPRT* Δ*uprt*::*gOMPDC*	Pru Δ*ku80* Δ*ompdc*::*HXGPRT*	This study

Strains, culture conditions, and PFU assays. The parental strains of *T. gondii* used in this study are Pru Δ*ku80*::*hxgprt* and Pru Δ*ku80* Δ*hxgprt* (17). The RH strain (38), designated the RH(EP) strain (39), was used as a virulent type I strain in challenge infections. All strains that were used or developed in this study are listed in Table 1. Parasites were maintained by serial passage in diploid human foreskin fibroblasts (HFF) at 35°C (40). PFU assays were performed over 8 days (41) unless otherwise stated. Uracil, uridine, cytidine, deoxyuridine, deoxycytidine, xanthine, mycophenolic acid (MPA), and 5-fluorodeoxyuridine (FUDR) were obtained from Sigma, Inc. 6-Thioxanthine (6TX) was obtained from Acros Organics (Thermo Fisher Scientific).

Pyrimidine starvation viability assays. Pyrimidine auxotrophs were serially diluted and inoculated into multiple 25-cm^2 HFF flasks. Parasites were allowed to invade for 2 h in uracil medium at 35°C, and cell monolayers were then rinsed 3× with cold phosphate-buffered saline (PBS) to remove uracil and extracellular parasites. Infected cultures were incubated for various periods of time without uracil to initiate uracil starvation conditions, and then uracil was added back to the culture medium at various times and PFU were scored 8 days later (18). The percentage of initial viability remaining after different times of uracil starvation was determined.

Genomic DNA isolation and PCR. Genomic DNA was purified using the DNA blood minikit (Qiagen). PCR products were amplified using a 4:1 mixture of Roche High Fidelity Expand Long and Expand Long *Taq* polymerases.

Transformation of *Toxoplasma gondii* and knockout verification strategy. Electroporations were performed on the model BTX600 electroporator with 1.33×10^7 freshly isolated tachyzoites in the presence of ~15 μg of linearized targeting plasmid DNA as described previously (17, 34, 37). Following selection of parasite clones, the genotype of the selected clones was validated in PCR assays to measure the following: (i) PCR 1, targeted deletion of the coding region of the targeted gene (DF and DR primers); (ii) PCR 2, correct targeted 5′ integration (CXF and 5′DHFRCXR primers); and (iii) PCR 3, correct targeted 3′ integration (3′DHFRCXF and CXR primers) using a previously described strategy (34).

Single and double knockouts at the *OMPDC* (Δ*ompdc*) and *UP* (Δ*up*) loci. The Pru Δ*ku80* Δ*hxgprt* strain was transfected with SpeI-linearized pOMPP4, or with SpeI-linearized pNUPP3, and knockouts were continuously selected in MPA (25 μg/ml), xanthine (250 μM), and uracil (250 μM) to select and isolate the cloned Pru Δ*ku80* Δ*ompdc*::*HXGPRT* and Pru Δ*ku80* Δ*up*::*HXGPRT* strains, respectively. To remove the *HXGPRT* minigene cassette from the Pru Δ*ku80* Δ*ompdc*::*HXGPRT*

strain, parasites were transfected with SpeI-linearized pOMPPC4 and selected in 6TX (250 μg/ml) and uracil (250 μM). The Pru Δ*ku80* Δ*ompdc* Δ*hxgprt* strain was validated using PCR 4 with a forward primer (CLOMF) designed into the 3′ side of the 5′ targeting flank and the CXR primer. The Pru Δ*ku80* Δ*ompdc* Δ*hxgprt* strain was transfected with SpeI-linearized pNUPP3 to isolate the Pru Δ*ku80* Δ*ompdc* Δ*up*::*HXGPRT* double mutant strain following selection in MPA and xanthine.

Functional complementation of the RH Δ*ku80* Δ*ompdc*::*HXGPRT* strain. The Pru Δ*ku80* Δ*ompdc*::*HXGPRT* strain was transfected with PmeI-linearized plasmid pgUPROMP containing the 3,258-bp genomic *OMPDC* gene. Following transfection, the culture was maintained in the presence of uracil (250 μM) for 24 h, and then uracil medium was removed, and the selection was continued in the absence of uracil. Parasites emerging from this selection were subcloned, and individual isolates were evaluated for their genotype to verify targeted deletion of *UPRT* and the simultaneous insertion of a functional allele of *OMPDC* at the *UPRT* locus. The genotype of the expected gene replacement at the *UPRT* locus was verified using PCR 5 to measure the deletion of the *UPRT* locus and by using PCR 6 and 7 to assay for correct 5′ and 3′ targeted integration of the genomic allele of *OMPDC* (using primers UPRTCXF with OMXEXR and OMXEXF with UPRTCXR). Individual clonal isolates were also examined for functional deletion of *UPRT* by measuring resistance to 50 μM FUDR to demonstrate loss of UPRT activity.

Mice, immunizations, T cell depletion, and challenge infections. Adult 6- to 8-week-old C57BL/6 and IFN-$\gamma^{-/-}$ knockout mice (002287) were obtained from The Jackson Laboratory (Bar Harbor, ME). Mice were maintained at the Dartmouth-Hitchcock Medical Center (Lebanon, NH) mouse facility, and mice were cared for and handled according to Animal Care and Use Program of Dartmouth College using National Institutes of Health-approved Institutional Animal Care and Use Committee guidelines. Mice were immunized twice 14 days apart with 3×10^6 tachyzoites by intraperitoneal injection. Purified anti-CD8 (clone 2.43) and isotype control (rat IgG2a) antibodies were purchased from BioXCell. Antibody (500 μg) was administered 1 day prior to challenge infections, and 250 μg of antibody was administered 0 and 3 days after challenge infection. $CD8^+$ T cells were depleted by greater than 99%. Challenge infections were performed 30 days after vaccination.

Cyst burden measurements. Brain cyst burdens were determined as previously described (33, 37). The Pru Δ*ku80* background expresses green fluorescent protein (GFP) under the control of a bradyzoite-specific *LDH2* promoter. Cysts were screened at ×150 magnification to detect GFP^+ bradyzoites encased within a cyst wall structure.

Statistical analysis. Unless noted otherwise, all experiments were repeated at least two times and results were similar between repeats. Statistical analysis was performed using Graphpad Prism 6 software. Data for PFU and cyst analysis was calculated using the 2-tailed unpaired Student *t* test. Student *t* tests were conducted under the assumption of equal variance. Survival experiments were analyzed using the log-rank Mantel-Cox test. A *P* value of <0.05 was considered to be statistically significant. *P* values of ≤ 0.05, 0.01, 0.001, or 0.0001 are indicated by *, **, ***, and ****, respectively, in Fig. 5 to 7.

RESULTS

Type II pyrimidine pathway mutants. To functionally define the predicted roles of the *de novo* pyrimidine synthesis and the pyrimidine salvage pathways (Fig. 1) in type II strains of *T. gondii*, we targeted the last enzymatic activity of the *de novo* pathway encoded by the orotidine monophosphate decarboxylase (*OMPDC*) gene that produces uridine-5′-monophosphate (UMP) from orotidine-5′-monophosphate to establish the pyrimidine nucleotide pool (14, 18). The Pru Δ*ku80* Δ*hxgprt* strain was targeted to delete the *OMPDC* gene to develop the Pru Δ*ku80* Δ*ompdc*::*HXGPRT* mutant (Fig. 2A). The uridine phosphorylase (*UP*) gene encodes the salvage enzyme that converts uridine or deoxyuridine to uracil

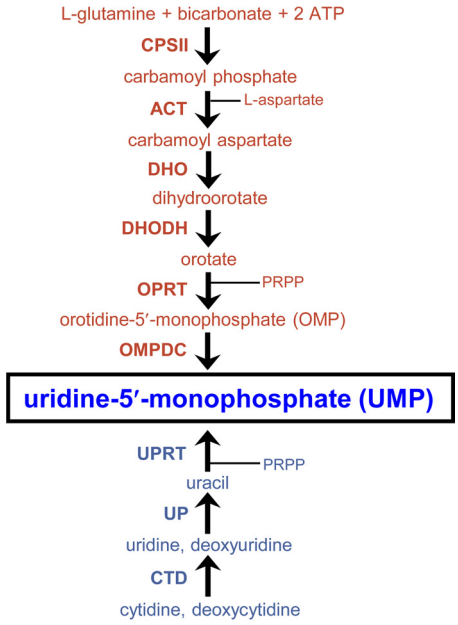

FIG 1 Pyrimidine synthesis and salvage pathways in *Toxoplasma gondii*. The six-step *de novo* pyrimidine synthesis pathway (red) and the pyrimidine salvage enzyme pathway (blue) show both pathways produce uridine-5′-monophosphate (UMP) (boxed). Intermediate metabolites are shown (phosphoribosyl-1-pyrophosphate [PRPP]). (Top) The biosynthetic enzymes mediating each step of the *de novo* pathway are carbamoyl phosphate synthetase II (CPSII), aspartate carbamoyltransferase (ACT), dihydroorotase (DHO), dihydroorotate dehydrogenase (DHODH), orotate phosphoribosyltransferase (OPRT), and orotidine-5′-monophosphate (OMP) decarboxylase (OMPDC). (Bottom) The pyrimidine salvage enzymes mediating each step of the salvage pathway are cytidine deaminase (CTD), uridine phosphorylase (UP), and uracil phosphoribosyltransferase (UPRT).

(42, 43) prior to its being salvaged into the nucleotide pool by conversion of uracil to UMP via the uracil phosphoribosyltransferase (UPRT) enzyme activity (Fig. 1) (39). The *UP* gene was deleted using a similar targeting strategy (Fig. 2A) to develop the Pru Δ*ku80* Δ*up*::*HXGPRT* mutant. The Pru Δ*ku80* Δ*ompdc*::*HXGPRT* mutant was then retargeted at the deleted *OMPDC* locus to excise the *HXGPRT* selectable marker to develop the Pru Δ*ku80* Δ*ompdc* Δ*hxgprt* mutant (Fig. 2B), which was retargeted to delete the *UP* locus to develop the Pru Δ*ku80* Δ*ompdc* Δ*up*::*HXGPRT* double mutant (Table 1). The Δ*ompdc* Δ*up* double mutant was developed to assess the ability of type II strains to salvage pyrimidine nucleosides from the host.

Functional analysis of pyrimidine synthesis and salvage in type II *T. gondii*. The type II Δ*ompdc*, Δ*up*, and Δ*ompdc* Δ*up* strains were examined in PFU assays under various growth conditions to assess parasite growth and nutrient rescue profiles. The Δ*up* mutant and the parental Pru Δ*ku80* strains replicate normally in the absence or in the presence of uracil, uridine, or cytidine (data not shown). In contrast, the type II Δ*ompdc* (Fig. 3A) and Δ*ompdc* Δ*up* (Fig. 3B) mutants exhibited a severe uracil auxotrophy and replication deficiency in the absence of uracil supplementation. In contrast to the complete rescue of growth observed with uracil supplementation (Fig. 3A and B), the replication of the Pru Δ*ompdc* mutant was only weakly rescued with high concentrations of uridine, as shown by the formation of very small plaques (Fig. 3C). In addition, the replication of the Pru Δ*ompdc* mutant

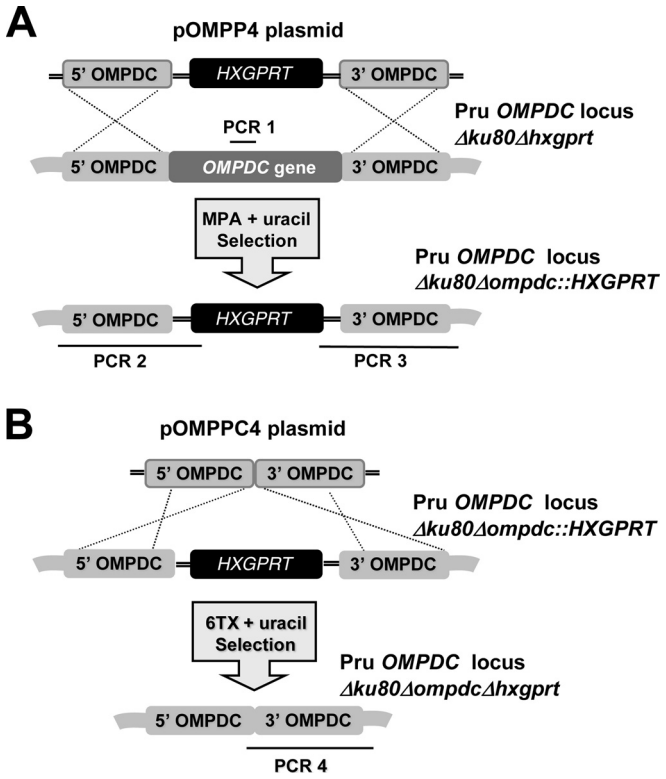

FIG 2 Targeted gene deletion at the orotidine 5′-monophosphate decarboxylase locus (*OMPDC*). (A) Strategy for deletion and validation of the endogenous *OMPDC* locus via targeted integration of the *HXGPRT* marker at the *OMPDC* locus of the Pru Δ*ku80* Δ*hxgprt* strain. Approximate locations of PCR products used to validate genotypes are depicted. The Pru Δ*ku80* Δ*hxgprt* parental strain was positive for the PCR 1 product, while the targeted *OMPDC* knockout was positive for PCR 2 and PCR 3 (see Materials and Methods). (B) Strategy for cleanup of the deleted *OMPDC* locus. The *HXGPRT* marker was removed from the disrupted OMPDC locus using the depicted strategy that utilized the ability to negatively select against the *HXGPRT* marker using 6TX selection. Successfully cleaned up strains with *HXGPRT* deleted were validated using PCR 4 (see Materials and Methods).

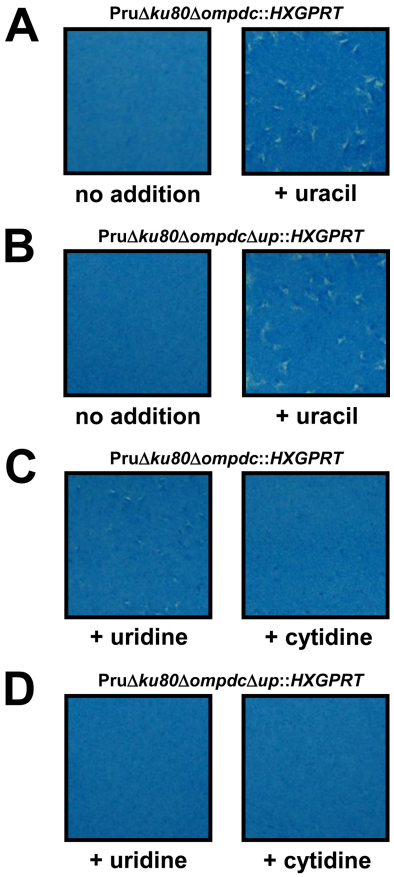

FIG 3 Functional rescue of type II *Toxoplasma gondii* uracil auxotrophs. Approximately 100 tachyzoites of the Pru Δ*ku80* Δ*ompdc*::*HXGPRT* (A and C) or Pru Δ*ku80* Δ*ompdc* Δ*up*::*HXGPRT* (B and D) strain were inoculated into a PFU assay in the absence of pyrimidine supplementation (A and B), in the presence of uracil supplementation (200 μM) (A and B), in the presence of uridine supplementation (200 μM) (C and D), or in the presence of cytidine supplementation (200 μM) (C and D) of the growth medium. The culture monolayer was stained 8 days later to reveal PFU and HFF monolayers.

was not significantly rescued in high concentrations of cytidine (Fig. 3C). Similar rescue profiles were observed using deoxyuridine and deoxycytidine, respectively (data not shown). The Pru Δ*ompdc* Δ*up* double mutant was not detectably rescued by addition of either uridine or cytidine (Fig. 3D), indicating that pyrimidine pathways in type II strains mirror the pathways known to exist in type I strains (18). However, the rescue of growth in type II strains using uridine or cytidine supplementation was reduced in comparison to rescue of the corresponding type I mutants, suggesting a reduced pyrimidine salvage capacity for pyrimidine nucleosides is present in type II strains.

Complementation of type II pyrimidine auxotrophy. The Pru Δ*ompdc* mutant was complemented by insertion of a functional wild-type allele of the *OMPDC* gene at the *UPRT* locus (Fig. 4A). The Pru Δ*ku80* Δ*ompdc*::*HXGPRT* Δ*uprt*::*gOMPDC* complemented strain was resistant to FUDR (data not shown), and the growth rate of the complemented strain was normal whether uracil was absent or present in the culture medium (Fig. 4B).

Pyrimidine starvation. PFU assays were used to measure how rapidly type II pyrimidine auxotrophs lost viability intracellularly under conditions of uracil starvation. When subjected to uracil starvation, the Pru Δ*ompdc* Δ*up* mutant lost viability at a markedly higher rate than the Pru Δ*ompdc* mutant (data not shown). In addition, the type II Pru Δ*ompdc* mutant lost viability at a significantly higher rate than the corresponding type I RH Δ*ompdc* mutant (Fig. 5).

Pyrimidine biosynthesis is required for type II virulence and cyst development. While the Pru Δ*ku80*::*HXGPRT* strain exhibits an ~75% lethal dose (LD_{75}) after a 2×10^5-tachyzoite challenge dose (Fig. 6A) and is uniformly lethal at higher doses (Fig. 6), C57BL/6 mice infected with the type II Pru Δ*ku80* Δ*ompdc*::*HXGPRT* mutant did not exhibit acute virulence or signs of infection after receiving challenge doses of 2×10^5 (Fig. 6A), 2×10^6 (Fig. 6B), or 2×10^7 (Fig. 6C) tachyzoites, and IFN-$\gamma^{-/-}$ knockout mice survived a 2×10^5 challenge dose (Fig. 6D). In contrast, the complemented Pru Δ*ku80* Δ*ompdc*::*HXGPRT* Δ*uprt*::*gOMPDC* strain exhibited the same acute virulence phenotype as the Pru Δ*ku80*::*HXGPRT* strain (Fig. 6).

Mice infected with 200 or 2×10^6 tachyzoites of the Pru Δ*ku80* Δ*ompdc*::*HXGPRT* mutant failed to establish detectable brain cyst burdens by 3 weeks postinfection (Fig. 6E). (Three weeks postinfection is the peak time point of cyst formation in the Pru Δ*ku80*

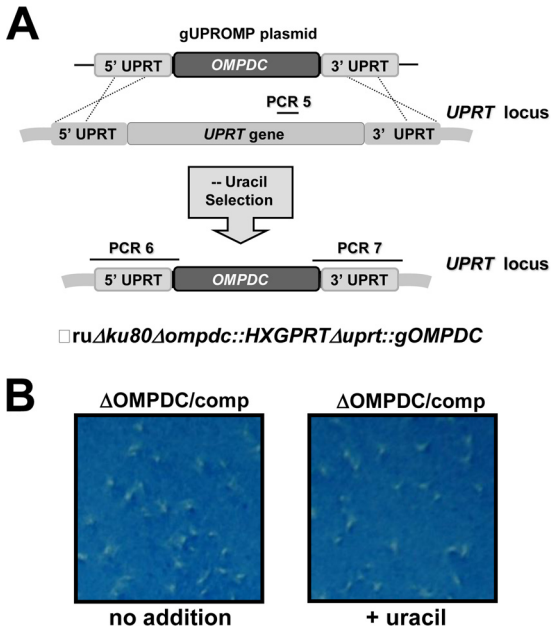

FIG 4 Complementation of the Pru Δ*ompdc* mutant. (A) Strategy for complementation of the Pru Δ*ompdc* mutant by simultaneous knockout of *UPRT* and targeted insertion of the genomic allele of *OMPDC* at the *UPRT* locus. The Pru Δ*ku80* Δ*ompdc*::*HXGPRT* strain was transfected with plasmid pGUPROMP and parasites that were complemented for *de novo* pyrimidine biosynthesis were selected by growth in media without uracil supplementation. Approximate locations of PCR validation product PCR 5 (targeted deletion of *UPRT*), and PCR 6 and PCR 7 (targeted integration of the genomic allele of *OMPDC*) are shown (see Materials and Methods). Correctly targeted replacement clones were positive for the PCR 6 and PCR 7 products and were negative for PCR 5. (B) Functional rescue of complemented strain Pru Δ*ku80* Δ*ompdc*::*HXGPRT* Δ*uprt*::*gOMPDC*. Approximately 100 tachyzoites of the Pru Δ*ku80* Δ*ompdc*::*HXGPRT* Δ*uprt*::*gOMPDC* strain were assayed in an 8-day PFU assay in the absence (no addition) or presence of uracil.

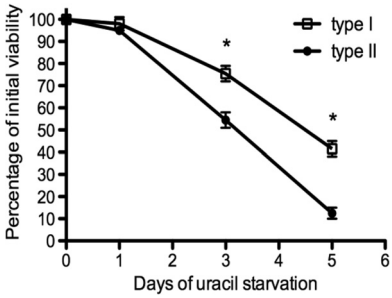

FIG 5 Pyrimidine starvation causes a rapid loss of parasite viability in type I and type II uracil auxotrophs. PFU assays were used to measure how rapidly pyrimidine auxotrophs lost viability intracellularly under conditions of pyrimidine starvation in a 5-day starvation assay. Viability profiles for the type II Pru Δ*ku80* Δ*ompdc*::*HXGPRT* mutant (solid circles) and the type I RH Δ*ku80* Δ*ompdc*::*HXGPRT* mutant (open squares) are shown. *, $P < 0.05$.

background [37].) Cysts were also not detected in mice infected with this mutant or the Pru Δ*ku80* Δ*ompdc* Δ*up*::*HXGPRT* double mutant at any time point evaluated up to 7 weeks postinfection (data not shown). In contrast, mice infected with 200 tachyzoites of the complemented Pru Δ*ku80* Δ*ompdc*::*HXGPRT* Δ*uprt*::*gOMPDC* strain exhibited typical cyst burdens compared to the Pru Δ*ku80*::*HXGPRT* strain (Fig. 6E). In addition, cysts were not detected in mice that survived the 2×10^7 challenge dose (Fig. 6C) of the Pru Δ*ku80* Δ*ompdc*::*HXGPRT* mutant (Fig. 6E). Collectively, these results demonstrate that type II uracil auxotroph mutants exhibit an avirulent phenotype and a severe defect in their ability to establish cysts and chronic infection.

Type II pyrimidine auxotrophs elicit protective immunity against type I and type II *T. gondii* infection. We examined type II pyrimidine auxotrophs as live attenuated vaccine strains. C57BL/6 mice were vaccinated with the Pru Δ*ku80* Δ*ompdc*::*HXGPRT* strain, and 30 days later, mice were challenged with 1,000 tachyzoites of virulent type I strain RH (LD1000) (Fig. 7A). All Pru Δ*ku80* Δ*ompdc*::*HXGPRT*-vaccinated mice survived type I virulent challenge infection, whereas no naive unvaccinated mice survived the challenge infection. We also evaluated protection from type II infection. Pru Δ*ku80* Δ*ompdc*::*HXGPRT*-vaccinated mice survived a type II virulent challenge of 2×10^7 tachyzoites, whereas no naive unvaccinated mice receiving this challenge dose survived (Fig. 7B). We performed $CD8^+$ T cell depletion experiments to determine whether this protective immunity was dependent on $CD8^+$ T cell populations. Vaccinated mice depleted of $CD8^+$ T cells rapidly succumbed to type II challenge infection, whereas vaccinated mice treated with control isotype antibody survived challenge infection (Fig. 7C). In addition, 31 days after type II challenge infection, we examined the brains of mice that survived type II challenge infection to assess whether brain cysts (chronic infection) were present. While naive mice that received a 200-tachyzoite challenge of the Pru Δ*ku80*::*HXGPRT* strain produced high numbers of cysts, cyst burdens were not detected in Pru Δ*ku80* Δ*ompdc*::*HXGPRT*-vaccinated mice that were rechallenged with 2×10^7 tachyzoites of the PruΔ *ku80*::*HXGPRT* strain (Fig. 7D).

DISCUSSION

Type I uracil auxotroph vaccines were previously described to stimulate potent T cell-mediated immunity to virulent type I challenge infection (15, 18, 19, 21–24). While the type I CPS uracil auxotroph vaccine also protected vaccinated mice from virulent type II challenge infection and reduced chronic infection (cyst burdens) by ~98%, vaccinated mice were incompletely protected from chronic infection (33). Our results using a nonreverting, nonreplicating, type II vaccine strain suggest that vaccination with a type II strain may provide a more secure immunity to type II infection by preventing cyst development and chronic infection. Type II uracil auxotroph vaccines protected mice from infection by both type I and type II strains.

Our investigation of pyrimidine auxotrophy in the type II background of *T. gondii* indicates that the pyrimidine synthesis and salvage pathways mirror the pathways previously reported in type I strains (14–16, 18). The uridine phosphorylase activity of type II is used to some extent for physiological salvage of uridine and deoxyuridine based on the observation of the formation of very small plaques when using either of these nucleosides to rescue the growth of the Pru Δ*ku80* Δ*ompdc*::*HXGPRT* vaccine strain. While visible plaques were observed in type I uracil auxotrophs using biochemical rescues with cytidine or deoxycytidine (18), visible plaques were not observed after cytidine or deoxycytidine rescue of the type II uracil auxotrophs in plaque assays. However, inspection of these cultures prior to staining did reveal tiny zones of infection involving just several infected cells without detectable

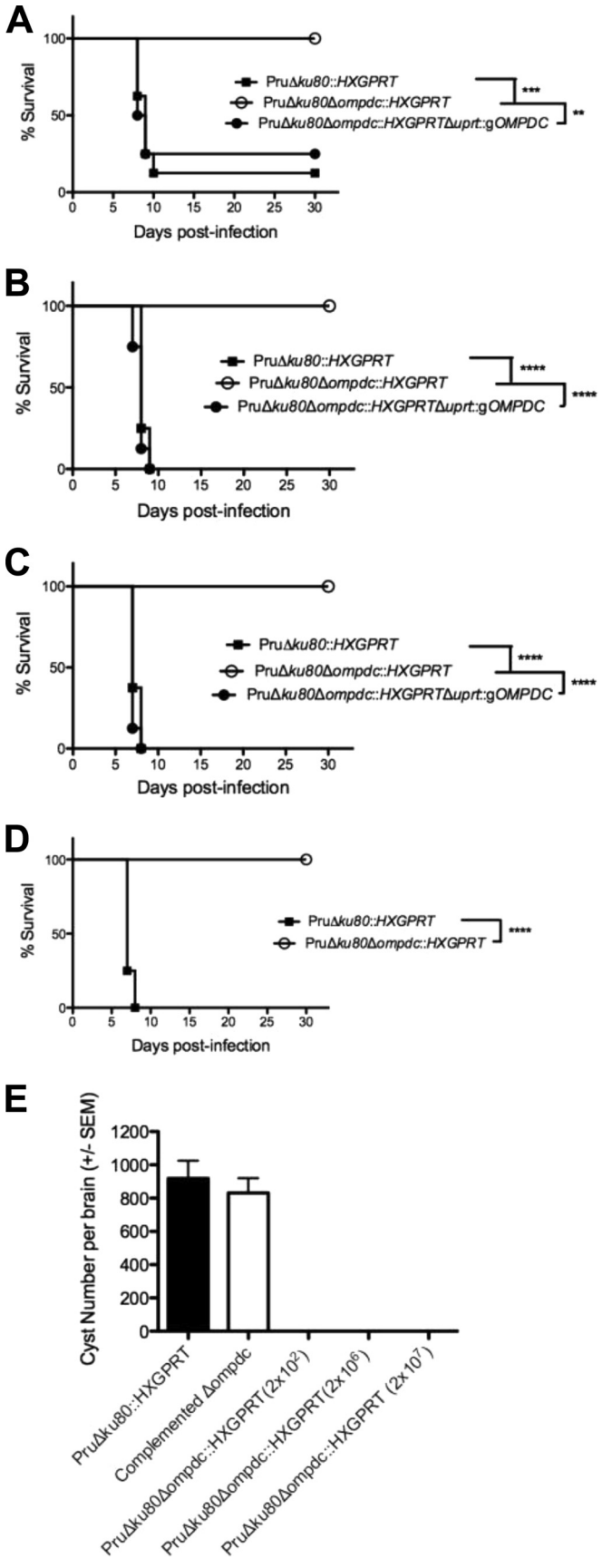

lysis of the monolayer. These results suggest that cytidine and deoxycytidine can be converted by type II strains into uridine or deoxyuridine, respectively, by the action of a cytidine deaminase activity. Nonetheless, the ability to rescue type II uracil auxotrophs with pyrimidine nucleosides was notably reduced in comparison to rescue profiles previously reported for type I uracil auxotrophs (18). In addition, we demonstrated that pyrimidine starvation also occurs at a higher rate in type II uracil auxotrophs than in corresponding type I mutants. Together, these results indicate that type II strains rely more heavily on the *de novo* pyrimidine synthesis pathway due to a reduced capacity to salvage pyrimidine nucleosides by comparison to type I uracil auxotroph mutants (18). While these findings may be explained by a reduced metabolic capacity at the cytidine deaminase, uridine phosphorylase, or uracil phosphoribosyltransferase steps of salvage (18), it is possible that this metabolic difference may also be affected by the inherent capacity of type I and type II strains to transport nutrients from the host cell into the vacuole or into the parasite, where nucleobases and nucleosides become available for incorporation into the UMP pool.

Deletion of *OMPDC* in the type II background of *T. gondii* induced a severe uracil auxotrophy, with loss of replication and loss of virulence in mice. Furthermore, cyst burdens and chronic infection were not established following high-dose infection or vaccination of mice with type II Δ*ompdc* uracil auxotroph mutants. Vaccination of mice with the Pru Δ*ku80* Δ*ompdc* mutant stimulated a fully protective $CD8^+$ T cell-dependent immunity that prevented virulent acute infection by type I and type II strains of *T. gondii*, and this vaccination also severely reduced or potentially prevented cyst formation after type II challenge infection in C57BL/6 mice. In our cyst burden analysis after challenge infections, we scored ~50% of the brain homogenates for cysts using dark-field microscopy to detect GFP^+ cysts. Extremely low-level cyst burdens may be present, although we estimate cyst burdens in rechallenged vaccinated mice to be below 1 cyst per brain.

Acute virulence in type I *T. gondii* uracil auxotrophs is attenuated by at least 8 logs (18), and type II uracil auxotroph virulence appears to be similarly attenuated. Type I uracil auxotrophs were previously demonstrated to elicit remarkably potent $CD4^+$ and $CD8^+$ T cell responses following vaccination of mice (15, 18-25, 27, 30-33). Consequently, nonreverting, nonreplicating, and non-cyst-forming Δ*ompdc* type II uracil auxotroph mutants provide new and improved vaccination tools to elicit protective immunity

FIG 6 Pyrimidine biosynthesis is required for type II virulence and cyst development. Groups ($n = 8$) of C57BL/6 mice were inoculated i.p. with (A) 2×10^5 tachyzoites, (B) 2×10^6 tachyzoites, or (C) 2×10^7 tachyzoites of the Pru Δ*ku80*::*HXGPRT* strain (solid squares), the Pru Δ*ku80* Δ*ompdc*::*HXGPRT* mutant (open circles), or the complemented Pru Δ*ku80* Δ*ompdc*::*HXGPRT* Δ*uprt*::g*OMPDC* strain (solid circles), and survival was monitored for 30 days. (D) IFN-$\gamma^{-/-}$ knockout mice ($n = 4$) were infected with 2×10^5 tachyzoites of the parental Pru Δ*ku80*::*HXGPRT* strain (solid squares) or the Pru Δ*ku80* Δ*ompdc*::*HXGPRT* mutant (open circles), and survival was monitored for 30 days (single experiment). (E) Cyst burdens in the brains of infected mice. Groups ($n = 8$) of mice were inoculated with 200 tachyzoites of the Pru Δ*ku80*::*HXGPRT* parental strain, with 200 tachyzoites of the complemented Pru Δ*ku80* Δ*ompdc*::*HXGPRT* Δ*uprt*::g*OMPDC* strain, or with 200 or 2×10^6 tachyzoites of the Pru Δ*ku80* Δ*ompdc*::*HXGPRT* mutant, and cyst burdens were determined 3 weeks postinfection. Cyst burdens were also determine in mice infected with 2×10^7 tachyzoites of the Pru Δ*ku80* Δ*ompdc*::*HXGPRT* mutant 31 days postinfection. **, $P < 0.01$; ***, $P < 0.001$; ****, $P < 0.0001$.

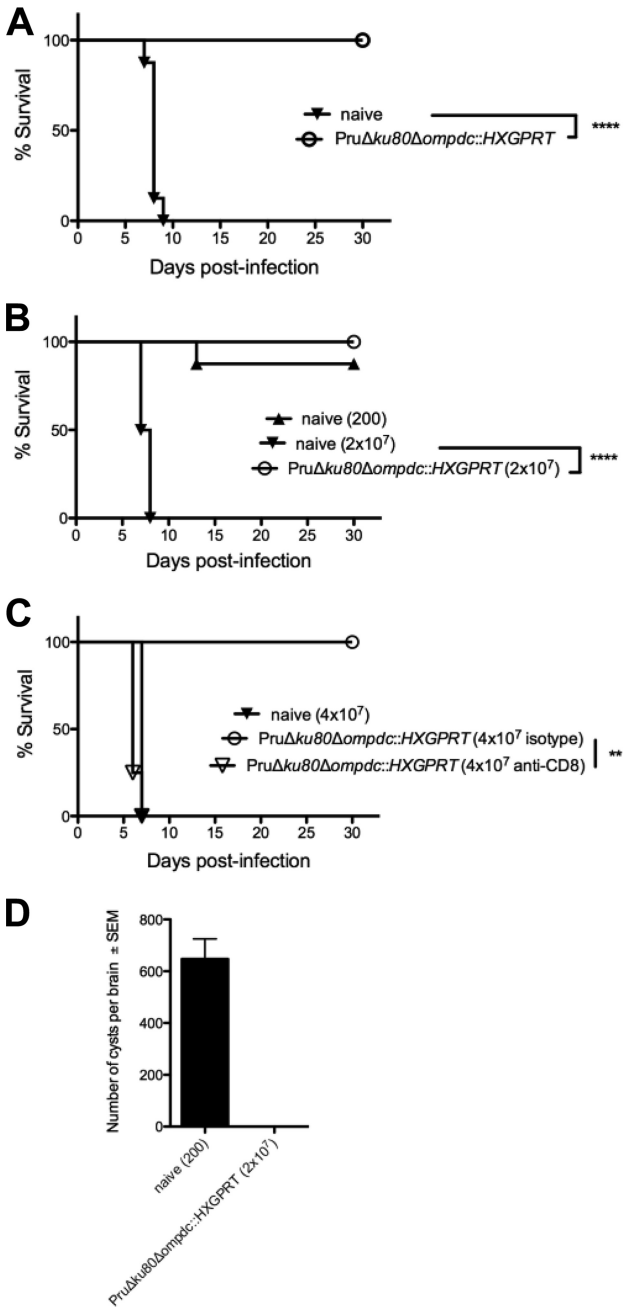

FIG 7 Type II uracil auxotrophs elicit protective immunity to type I and type II *T. gondii* infection. Groups of C57BL/6 mice ($n = 8$) were vaccinated with the type II Pru Δ*ku80* Δ*ompdc*::*HXGPRT* mutant, or groups of mice were left unvaccinated (naive). Mice were challenged with type I (RH) or type II (Pru Δ*ku80*::*HXGPRT*) infections 30 days after vaccination, and survival was monitored for 30 days. (A) Pru Δ*ku80* Δ*ompdc*::*HXGPRT* mutant-vaccinated mice (○) or unvaccinated naive mice (▼) were challenged i.p. with 1000 tachyzoites of the virulent type I RH strain. (B) Pru Δ*ku80* Δ*ompdc*::*HXGPRT* mutant-vaccinated mice (○) or unvaccinated naive mice were challenged intraperitoneally with 200 (▲) or 2×10^7 (▼) tachyzoites of the type II Pru Δ*ku80*::*HXGPRT* strain. (C) Naive or vaccinated mice ($n = 4$), as indicated, were treated with anti-CD8 antibody or isotype control antibody at the time of challenge infection with 4×10^7 type II Pru Δ*ku80*::*HXGPRT* tachyzoites. (D) Cyst burdens present in the brains of Pru Δ*ku80* Δ*ompdc*::*HXGPRT* mutant-vaccinated mice that were rechallenged with 2×10^7 tachyzoites of the Pru Δ*ku80*::*HXGPRT* strain ($n = 8$) or present in naive mice that were challenged with 200 tachyzoites of the Pru Δ*ku80*::*HXGPRT* strain ($n = 7$). Cyst measurements were performed 31 days postinfection. **, $P < 0.01$; ****, $P < 0.0001$.

to *T. gondii* and to examine the host immune responses that are elicited by vaccination with a live attenuated type II vaccine strain.

ACKNOWLEDGMENTS

This work was supported by NIH grants AI041930, AI097018, and AI105563. ToxoDB, PlasmoDB, and EuPathDB are part of the NIH/NIAID-funded Bioinformatics Resource Center.

The valuable work of the developers of the *Toxoplasma gondii* Genome Resource at www.ToxoDB.org is gratefully acknowledged.

REFERENCES

1. **Dubey JP.** 2007. The history and life cycle of *Toxoplasma gondii*, p 1-18. *In* Weiss LM, Kim K (ed), *Toxoplasma gondii*: the model apicomplexan parasite: perspectives and methods. Elsevier, London, United Kingdom.
2. **Jones JL, Kruszon-Moran D, Wilson M, McQuillan G, Navin T, McAuley JB.** 2001. *Toxoplasma gondii* infection in the United States: seroprevalence and risk factors. Am J Epidemiol **154:**357–365. http://dx.doi.org/10.1093/aje/154.4.357.
3. **Howe DK, Sibley LD.** 1995. *Toxoplasma gondii* comprises three clonal lineages: correlation of parasite genotype with human disease. J Infect Dis **172:**1561–1566. http://dx.doi.org/10.1093/infdis/172.6.1561.
4. **Weiss LM, Kim K.** 2000. The development and biology of bradyzoites of *Toxoplasma gondii*. Front Biosci **5:**D391–D405. http://dx.doi.org/10.2741/Weiss.
5. **Denkers EY, Bzik DJ, Fox BA, Butcher BA.** 2012. An inside job: hacking into JAK/STAT signaling cascades by the intracellular protozoan *Toxoplasma gondii*. Infect Immun **80:**476–482. http://dx.doi.org/10.1128/IAI.05974-11.
6. **Dubey JP, Lindsay DS, Speer CA.** 1998. Structures of *Toxoplasma gondii* tachyzoites, bradyzoites, and sporozoites and biology and development of tissue cysts. Clin Microbiol Rev **11:**267–299.
7. **Luft BJ, Remington JS.** 1992. Toxoplasmic encephalitis in AIDS. Clin Infect Dis **15:**211–222. http://dx.doi.org/10.1093/clinids/15.2.211.
8. **Jones JL, Holland GN.** 2010. Annual burden of ocular toxoplasmosis in the US. Am J Trop Med Hyg **82:**464–465. http://dx.doi.org/10.4269/ajtmh.2010.09-0664.
9. **Zhang NZ, Chen J, Wang M, Petersen E, Zhu XQ.** 2013. Vaccines against *Toxoplasma gondii*: new developments and perspectives. Expert Rev Vaccines **12:**1287–1299. http://dx.doi.org/10.1586/14760584.2013.844652.
10. **Butcher BA, Denkers EY.** 2002. Mechanism of entry determines the ability of *Toxoplasma gondii* to inhibit macrophage proinflammatory cytokine production. Infect Immun **70:**5216–5224. http://dx.doi.org/10.1128/IAI.70.9.5216-5224.2002.
11. **Subauste CS, Wessendarp M.** 2000. Human dendritic cells discriminate between viable and killed *Toxoplasma gondii* tachyzoites: dendritic cell activation after infection with viable parasites results in CD28 and CD40 ligand signaling that controls IL-12-dependent and -independent T cell production of IFN-gamma. J Immunol **165:**1498–1505. http://dx.doi.org/10.4049/jimmunol.165.3.1498.
12. **Dupont CD, Christian DA, Hunter CA.** 2012. Immune response and immunopathology during toxoplasmosis. Semin Immunopathol **34:**793–813. http://dx.doi.org/10.1007/s00281-012-0339-3.
13. **Dzierszinski FS, Hunter CA.** 2008. Advances in the use of genetically engineered parasites to study immunity to *Toxoplasma gondii*. Parasite Immunol **30:**235–244. http://dx.doi.org/10.1111/j.1365-3024.2007.01016.x.
14. **Fox BA, Chaudhary K, Bzik DJ.** 2007. *Toxoplasma*: molecular and cellular biology. Horizon Bioscience, Norwich, United Kingdom.
15. **Fox BA, Bzik DJ.** 2002. De novo pyrimidine biosynthesis is required for virulence of *Toxoplasma gondii*. Nature **415:**926–929. http://dx.doi.org/10.1038/415926a.
16. **Fox BA, Ristuccia JG, Bzik DJ.** 2009. Genetic identification of essential indels and domains in carbamoyl phosphate synthetase II of *Toxoplasma gondii*. Int J Parasitol **39:**533–539. http://dx.doi.org/10.1016/j.ijpara.2008.09.011.
17. **Fox BA, Ristuccia JG, Gigley JP, Bzik DJ.** 2009. Efficient gene replacements in *Toxoplasma gondii* strains deficient for nonhomologous end joining. Eukaryot Cell **8:**520–529. http://dx.doi.org/10.1128/EC.00357-08.
18. **Fox BA, Bzik DJ.** 2010. Avirulent uracil auxotrophs based on disruption of orotidine-5′-monophosphate decarboxylase elicit protective immunity to *Toxoplasma gondii*. Infect Immun **78:**3744–3752. http://dx.doi.org/10.1128/IAI.00287-10.

19. **Gigley JP, Fox BA, Bzik DJ.** 2009. Cell-mediated immunity to *Toxoplasma gondii* develops primarily by local Th1 host immune responses in the absence of parasite replication. J Immunol **182:**1069–1078. http://dx.doi.org/10.4049/jimmunol.182.2.1069.
20. **Baird JR, Byrne KT, Lizotte PH, Toraya-Brown S, Scarlett UK, Alexander MP, Sheen MR, Fox BA, Bzik DJ, Bosenberg M, Mullins DW, Turk MJ, Fiering S.** 2013. Immune-mediated regression of established B16F10 melanoma by intratumoral injection of attenuated *Toxoplasma gondii* protects against rechallenge. J Immunol **190:**469–478. http://dx.doi.org/10.4049/jimmunol.1201209.
21. **Dupont CD, Christian DA, Selleck EM, Pepper M, Leney-Greene M, Harms Pritchard G, Koshy AA, Wagage S, Reuter MA, Sibley LD, Betts MR, Hunter CA.** 2014. Parasite fate and involvement of infected cells in the induction of $CD4^+$ and $CD8^+$ T cell responses to *Toxoplasma gondii*. PLoS Pathog **10:**e1004047. http://dx.doi.org/10.1371/journal.ppat.1004047.
22. **Jordan KA, Wilson EH, Tait ED, Fox BA, Roos DS, Bzik DJ, Dzierszinski F, Hunter CA.** 2009. Kinetics and phenotype of vaccine-induced $CD8^+$ T-cell responses to *Toxoplasma gondii*. Infect Immun **77:**3894–3901. http://dx.doi.org/10.1128/IAI.00024-09.
23. **Shaw MH, Freeman GJ, Scott MF, Fox BA, Bzik DJ, Belkaid Y, Yap GS.** 2006. Tyk2 negatively regulates adaptive Th1 immunity by mediating IL-10 signaling and promoting IFN-gamma-dependent IL-10 reactivation. J Immunol **176:**7263–7271. http://dx.doi.org/10.4049/jimmunol.176.12.7263.
24. **Sukhumavasi W, Egan CE, Warren AL, Taylor GA, Fox BA, Bzik DJ, Denkers EY.** 2008. TLR adaptor MyD88 is essential for pathogen control during oral *Toxoplasma gondii* infection but not adaptive immunity induced by a vaccine strain of the parasite. J Immunol **181:**3464–3473. http://dx.doi.org/10.4049/jimmunol.181.5.3464.
25. **Wilson DC, Matthews S, Yap GS.** 2008. IL-12 signaling drives $CD8^+$ T cell IFN-gamma production and differentiation of $KLRG1^+$ effector subpopulations during *Toxoplasma gondii* infection. J Immunol **180:**5935–5945. http://dx.doi.org/10.4049/jimmunol.180.9.5935.
26. **Wilson DC, Grotenbreg GM, Liu K, Zhao Y, Frickel EM, Gubbels MJ, Ploegh HL, Yap GS.** 2010. Differential regulation of effector- and central-memory responses to *Toxoplasma gondii* infection by IL-12 revealed by tracking of Tgd057-specific $CD8^+$ T cells. PLoS Pathog **6:**e1000815. http://dx.doi.org/10.1371/journal.ppat.1000815.
27. **Dzierszinski F, Pepper M, Stumhofer JS, LaRosa DF, Wilson EH, Turka LA, Halonen SK, Hunter CA, Roos DS.** 2007. Presentation of *Toxoplasma gondii* antigens via the endogenous major histocompatibility complex class I pathway in nonprofessional and professional antigen-presenting cells. Infect Immun **75:**5200–5209. http://dx.doi.org/10.1128/IAI.00954-07.
28. **Goldszmid RS, Coppens I, Lev A, Caspar P, Mellman I, Sher A.** 2009. Host ER-parasitophorous vacuole interaction provides a route of entry for antigen cross-presentation in *Toxoplasma gondii*-infected dendritic cells. J Exp Med **206:**399–410. http://dx.doi.org/10.1084/jem.20082108.
29. **Gubbels MJ, Striepen B, Shastri N, Turkoz M, Robey EA.** 2005. Class I major histocompatibility complex presentation of antigens that escape from the parasitophorous vacuole of *Toxoplasma gondii*. Infect Immun **73:**703–711. http://dx.doi.org/10.1128/IAI.73.2.703-711.2005.
30. **Baird JR, Fox BA, Sanders KL, Lizotte PH, Cubillos-Ruiz JR, Scarlett UK, Rutkowski MR, Conejo-Garcia JR, Fiering S, Bzik DJ.** 2013. Avirulent *Toxoplasma gondii* generates therapeutic antitumor immunity by reversing immunosuppression in the ovarian cancer microenvironment. Cancer Res **73:**3842–3851. http://dx.doi.org/10.1158/0008-5472.CAN-12-1974.
31. **Fox BA, Sanders KL, Bzik DJ.** 2013. Non-replicating *Toxoplasma* reverses tumor-associated immunosuppression. Oncoimmunology **2:**e26296. http://dx.doi.org/10.4161/onci.26296.
32. **Fox BA, Sanders KL, Chen S, Bzik DJ.** 2013. Targeting tumors with nonreplicating *Toxoplasma gondii* uracil auxotroph vaccines. Trends Parasitol **29:**431–437. http://dx.doi.org/10.1016/j.pt.2013.07.001.
33. **Gigley JP, Fox BA, Bzik DJ.** 2009. Long-term immunity to lethal acute or chronic type II *Toxoplasma gondii* infection is effectively induced in genetically susceptible C57BL/6 mice by immunization with an attenuated type I vaccine strain. Infect Immun **77:**5380–5388. http://dx.doi.org/10.1128/IAI.00649-09.
34. **Rommereim LM, Hortua Triana MA, Falla A, Sanders KL, Guevara RB, Bzik DJ, Fox BA.** 2013. Genetic manipulation in Deltaku80 strains for functional genomic analysis of *Toxoplasma gondii*. J Vis Exp e50598. http://dx.doi.org/10.3791/50598.
35. **Donald RG, Carter D, Ullman B, Roos DS.** 1996. Insertional tagging, cloning, and expression of the *Toxoplasma gondii* hypoxanthine-xanthine-guanine phosphoribosyltransferase gene. Use as a selectable marker for stable transformation. J Biol Chem **271:**14010–14019.
36. **Donald RG, Roos DS.** 1998. Gene knock-outs and allelic replacements in *Toxoplasma gondii*: HXGPRT as a selectable marker for hit-and-run mutagenesis. Mol Biochem Parasitol **91:**295–305. http://dx.doi.org/10.1016/S0166-6851(97)00210-7.
37. **Fox BA, Falla A, Rommereim LM, Tomita T, Gigley JP, Mercier C, Cesbron-Delauw MF, Weiss LM, Bzik DJ.** 2011. Type II *Toxoplasma gondii* KU80 knockout strains enable functional analysis of genes required for cyst development and latent infection. Eukaryot Cell **10:**1193–1206. http://dx.doi.org/10.1128/EC.00297-10.
38. **Sabin AB.** 1941. Toxoplasmic encephalitis in children. JAMA **116:**801–807. http://dx.doi.org/10.1001/jama.1941.02820090001001.
39. **Pfefferkorn ER.** 1978. *Toxoplasma gondii*: the enzymic defect of a mutant resistant to 5-fluorodeoxyuridine. Exp Parasitol **44:**26–35. http://dx.doi.org/10.1016/0014-4894(78)90077-2.
40. **Fox BA, Gigley JP, Bzik DJ.** 2004. *Toxoplasma gondii* lacks the enzymes required for de novo arginine biosynthesis and arginine starvation triggers cyst formation. Int J Parasitol **34:**323–331. http://dx.doi.org/10.1016/j.ijpara.2003.12.001.
41. **Pfefferkorn ER, Pfefferkorn LC.** 1976. *Toxoplasma gondii*: isolation and preliminary characterization of temperature-sensitive mutants. Exp Parasitol **39:**365–376. http://dx.doi.org/10.1016/0014-4894(76)90040-0.
42. **Iltzsch MH.** 1993. Pyrimidine salvage pathways in *Toxoplasma gondii*. J Eukaryot Microbiol **40:**24–28. http://dx.doi.org/10.1111/j.1550-7408.1993.tb04877.x.
43. **Iltzsch MH, Klenk EE.** 1993. Structure-activity relationship of nucleobase ligands of uridine phosphorylase from *Toxoplasma gondii*. Biochem Pharmacol **46:**1849–1858. http://dx.doi.org/10.1016/0006-2952(93)90592-K.